Full Length Article

# Fate of mercury in two CFB utility boilers with different fueled coals and air pollution control devices

Xinyu Li[a,b], Zhonggen Li[a,*], Chengcheng Fu[c], Li Tang[a], Ji Chen[a], Tingting Wu[a], Che-Jen Lin[a,d,e], Xinbin Feng[a,*], Xuewu Fu[a]

[a] State Key Laboratory of Environmental Geochemistry, Institute of Geochemistry, Chinese Academy of Sciences, Guiyang 550081, China
[b] University of Chinese Academy of Sciences, Beijing 100049, China
[c] Guizhou Environmental Monitoring Center, Guiyang 550081, China
[d] Center for Advances in Water and Air Quality, Lamar University, Beaumont, TX 77710, USA
[e] Department of Civil and Environmental Engineering, Lamar University, Beaumont, TX 77710, USA

ABSTRACT

Mercury (Hg) emitted from two circulating fluidized bed (CFB) utility boilers (150 MW, P#1 and 300 MW, P#2) in Guizhou province, Southwest China, was characterized. P#1 used anthracite coal and was equipped with in-furnace desulfurization (IFD) and electrostatic precipitator (ESP). P#2 co-burned gangue and coal slime and was equipped with selective non-catalytic reduction (SNCR), ESP, fabric filter (FF) and limestone gypsum wet flue gas desulfurization (WFGD). Flue gas samples from the inlets and outlets of air pollution control devices (APCDs) in the two plants were analyzed using the Ontario Hydro Method (OHM). Solid samples including feed coal, limestone, bottom ash, fly ash and gypsum were also collected and analyzed. Hg removal efficiency by the APCDs and Hg emission factors (MEFs) were estimated. Total Hg (THg) in the flue gas at the inlet of ESP are 32.3 $\mu g \cdot m^{-3}$ and 15.3 $\mu g \cdot m^{-3}$ for P#1 and P#2, respectively, both dominated (95.11–99.26%) by the particulate form (Hg$^p$). THg decreased significantly to 0.19–0.24 $\mu g \cdot m^{-3}$ at the final APCDs outlets of these two power plants, yielding an overall Hg removal efficiency of 98.53–99.41% for THg. Mass balance analysis indicated that > 97% of Hg in coals ended up in captured fly ash. MEFs of the two tested power plants are relatively lower than the values typically found in CFB and pulverized coal (PC) utility boiler power plants. The emission data of Hg from CFB coal-fired power plants should be updated and attention should be directed to the secondary emission/release of Hg from the captured fly ash.

## 1. Introduction

Hg, with its toxicity, environmental persistence, atmospheric transport and bioaccumulation, has been listed as a priority pollutant worldwide [1,2]. Anthropogenic Hg emissions exceeded that of natural sources gradually and became the main origin of Hg in the global environment after the industrial revolution [3–5]. The massive Hg emission into the atmosphere has caused adverse effects on the ecological environment [1], such as the obvious accumulation of Hg in different environmental media around the emission source, including soil/sediment, vegetables and grains [6–9]. Asia is the most important region of Hg emissions in the world during the past three decades [1,5,10–11], with China contributing to approximately 1/4 of global anthropogenic emission [5,12,13]. The Hg emissions from coal combustion, lead/zinc smelting and cement industry had become the main Hg contributing

sources in China in recent years [13,14].

Circulating fluidized bed (CFB) boiler and pulverized coal (PC) boiler are two major boilers of power plants. As a clean combustion technology, the CFB boiler has a wider fuel adaptability, higher combustion efficiency, lower pollutant emission and lower cost than that of PC boiler, resulting in extensive application in many cases [15]. China has the largest installed capacity of CFB boilers in the world, with more than 281 CFB boilers (installed capacity > 150 MW) in operation [16]. As for 2015, CFB boilers accounted for 10% of the total installed capacity in coal-fired power plants [17]. Hg released from coal combustion is an important source of anthropogenic Hg. Dai et al. [18] estimated the average Hg concentration in coal burned in China is 0.16 $mg \cdot kg^{-1}$ (N = 1666), and the world average value for Hg in coal is only 0.10 $mg \cdot kg^{-1}$ [19]. Coal combustion in power plants and industrial boilers is still the most dominant source of Hg emissions in

China [13,14,20].

Coal-fired power plants are among the top priority sources to be controlled in the Minamata Convention on Mercury. As the largest anthropogenic Hg emission source in China, it is particularly important to continuously update the quantity and emission factors of Hg emissions in coal-fired power plants [14]. Given the advantages of CFB boiler, it's installations in China has been widely applied for new plants. However, Hg emission characteristics in CFB facilities have not been studied as extensively as those with PC boilers. Furthermore, technological progress of CFB boilers and air pollution control devices (APCDs) implementation also facilitate the need for updating of Hg emissions in this field. Most earlier studies measured total Hg (THg) content in flue gas or calculated the removal rate and emission factor of Hg [21–23]. There were few investigations focused on Hg emission speciation in the flue gas from CFB facilities [24]. Also earlier works showed diverse results because Hg concentration in coal had regional differences and the combination of APCDs were different in CFB power plants. Therefore, more onsite emission measurements of Hg from CFB boilers are urgent needed to reduce the uncertainties of anthropogenic Hg emission estimate from this source.

Guizhou has one of the largest coal reserves among the provinces in China and has incentives for coal-energy development [25]. In the past 20 years, coal-fired power plants have been greatly expanded in the province because of the west-to-east power transmission project. In addition, the CFB boilers were also applied in industrial production. In this study, the characteristics of atmospheric Hg emission, including emission quantity and speciation, at two CFB power plants in Guizhou that used different kind of coal or coal processing byproducts, along with different APCDs, were investigated. Based on the sampling and analyzing of flue gas using the Ontario Hydro Method (OHM), and analysis of Hg concentration in different input/output solid samples, Hg removal efficiency through APCDs and mercury atmospheric emission were calculated. The study updates mercury emission factor (MEF) of CFB boilers in China and provides directions for future study of this source.

## 2. Methodology

### 2.1. Power plants description and sampling sites

Guizhou Province, situated in southwest China, reserves large amounts of coal resources [25]. The studied two CFB power plants are located in the western and southwestern Guizhou for power plant #1 (P#1) and power plant #2 (P#2), respectively. The configuration of APCDs and the sampling locations of these two power plants were showed in Table 1 and Fig. 1. P#1 has two 150-MW CFB boilers equipped with in-furnace desulfurization (IFD) and electrostatic precipitator (ESP). P#2 has two 300-MW CFB boilers with selective non-catalytic reduction (SNCR), ESP, fabric filter (FF) and limestone gypsum wet flue gas desulfurization (WFGD). The fuel used in P#1 is anthracite coal and that of P#2 is gangue and coal slime from coal preparation plant, all fuels were from local area where the power plant located. Flue gas samples were collected at the ESP inlet and ESP outlet in P#1 and the ESP inlet and WFGD outlet in P#2, respectively (Fig. 1).

### 2.2. Sampling and analysis methods

The Ontario Hydro Method (OHM) (ASTM Method 6784-02, 2008) was applied to sample gaseous elemental mercury ($Hg^0$), gaseous oxidized mercury ($Hg^{2+}$) and particulate mercury ($Hg^p$) in the flue gas by equipment of Model XC-572 (Apex Instruments, USA). $Hg^p$ was first collected on the glass fiber filter, and an additional glass cyclone was used before the glass fiber filter when the flue gas contained too much particulate matter (PM) at locations such as ESP/FF inlet in this study. Three impingers each containing 100 mL KCl solution (1 mol·$L^{-1}$) were then used to capture $Hg^{2+}$. One impinge with $H_2O_2$ + $HNO_3$ (100 mL, 10% v/v + 5% v/v) and three impingers with $H_2SO_4$ + $KMnO_4$ solution (100 mL, 10% v/v + 4% m/v) jointly collected $Hg^0$ through oxidation and absorption processes. In the end, an impinger with silica gel was used to remove moisture in flue gas. Both the probe and the filters were heated to at least 120 °C to avoid the water condensation and Hg adsorption on the tubing walls. Each flue gas sampling ran lasted for 1–1.5 h. Hg samples collected in the scavenging solutions were reduced by $SnCl_2$, and measured 2-X times by Cold Vapor Atomic Absorption Spectrophotometry (CVAAS, F732S, Shanghai Huaguang Instrument Corp), which had an instrument detection limit of 0.05 µg·$L^{-1}$.

Solid materials including fuel (coal, gangue and coal slime), bottom ash, fly ash, limestone and gypsum were collected simultaneously during the flue gas sampling. After drying at 40 °C for 3–7 days and grinding to < 0.150 mm, Hg concentrations in solid samples, including the glass fiber filters, were determined using the US EPA Method 7473. The method heats solid samples at 800 °C and measured the released $Hg^0$ by CVAAS (Lumex RA915+, Russia) with a method detection limit of 0.1 µg·$kg^{-1}$. Each solid sample was determined at least three times to obtain a mean Hg value. Proximate analysis of feed fuels was performed using the Chinese national standard method (GB/T 212-2008). Ultimate analysis (carbon, nitrogen and hydrogen) was determined by an elemental analyzer (vario MACRO cube, Elementar, Germany). Un-burned carbon (UBC) content in fly ash samples was also determined by the elemental analyzer. Total sulfur was detected by the Eschka method following GB/T 214-2007. The calorific value was determined using GB/T 213-2008.

### 2.3. Quality assurance and quality control

Materials used for flue gas sampling were carefully pretreated before each field work to reduce the system blank and possible contamination. Quartz filters for collecting $Hg^p$ were heated for 2 h at 500 °C. Teflon tubing was cleaned using 20% nitric acid ($HNO_3$), impingers and bottles were soaked into a 20% $HNO_3$ overnight, and then washed with deionized water before sampling. For Hg analysis, certified reference materials of coal (NIST SRM 1632d), fly ash (NIST SRM 1633c; GBW 08401), dolomite (JDo-1) and soil (GSS-5) were measured to guarantee the analytical quality. The difference between measured Hg and the recommended values was found to be less than 10%, such as the observed Hg concentrations in NIST SRM 1632d, NIST SRM 1633c, GBW08401, JDo-1, GSS-5 were 87 ± 8 (N = 7), 929 ± 137 (N = 5), 36 ± 2 (N = 6), 8.9 ± 1.5 (N = 3), 282 ± 27(N = 10) µg·$kg^{-1}$, respectively, versus to the recommended values: 92.8 ± 3.3, 1005 ± 22, 39, 9.5 and 290 ± 30 µg·$kg^{-1}$, respectively. For proximate and ultimate analysis, the concentrations of certified reference materials (GSB06-2105-2007 for anthracite and GSB06-2182-2008-1

**Table 1**
Information on the studies CFB power plants and flue gas sampling locations.

| Power plants | Boiler types | Installed capacity (MW) | APCDs[*] | Flue gas sampling locations |
|---|---|---|---|---|
| P#1 | CFB | 2 × 150 MW | IFD + ESP | ESP inlet and outlet |
| P#2 | CFB | 2 × 300 MW | SNCR + ESP-FF + WFGD | ESP-FF inlet and WFGD outlet |

* IFD: In-furnace desulphurization; ESP: Electrostatic precipitator; SNCR: Selective non-catalytic reduction; FF: Fabric filter; WFGD: Wet flue gas desulphurization.
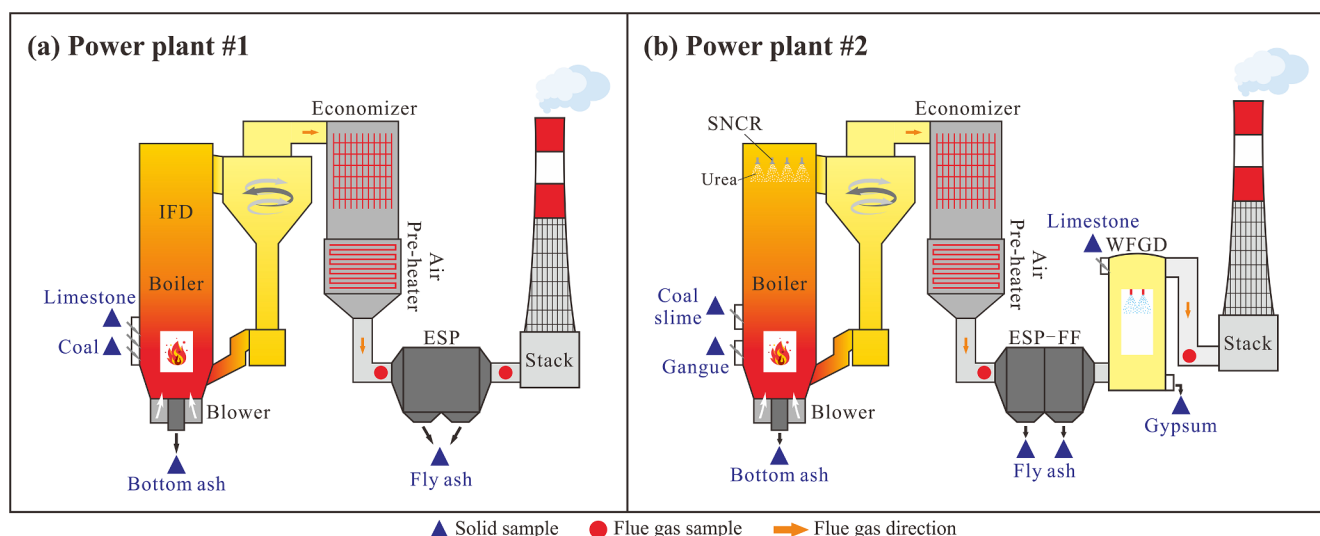
**Fig. 1.** Schematics of the two CFB power plants and the sampling locations.

for gangue) were measured with feed fuel samples (gangue, coal slime and coal). The means of measured compositions were within 5% of deviation from the certified contents.

## 3. Results and discussion

### 3.1. Fuel analysis

Proximate and ultimate analysis in fuels from the two plants are shown in Table 2. All feed coal samples were classified into middle to low calorific value coal according to GB 15224.3-2010 (16.7–21.3 MJ·kg$^{-1}$), since their calorific values were in the range of 17.03–19.66 MJ·kg$^{-1}$. The moisture content of coal slime (9.06%) was higher than that of other fuels (2.52–2.89%) and the volatiles of coal in P#1 (10.41%) was lower than that of P#2 (17.53–18.77%). Based on the National Coal Classification Standard of China (GB 15224.1-2010 and GB 15224.2-2010), the fuel in P#1 was classified as high-ash (39.62%) and high-sulfur (3.05%) coal, and the fuel in P#2 was extra-high-ash (43.94–45.15%) and low-sulfur (0.29–0.45%) coal. In summary, fuels in this study were of relatively high-ash and low-calorific values compared to typical coals used in PC boiler power plants [26,27], but were similar to feed coals used in six other CFB boilers in Shanxi province, China [21].

### 3.2. Mercury in solid samples

Hg concentration of coal in P#1 was 233 $\pm$ 39 μg·kg$^{-1}$ (Table 3), exceeding the mean content in coal from China (163 μg·kg$^{-1}$) [18] and the world average value of Hg in coal (0.10 mg·kg$^{-1}$) [19]. Gangue and coal slime in P#2 had Hg content of 113 $\pm$ 23 μg·kg$^{-1}$ and 65 $\pm$ 20 μg·kg$^{-1}$, respectively. The different Hg concentrations in these two plants may be related to the sulfur content since Hg in coal

were associated with sulfur in coal in most cases [28]. The limestone had low concentrations of Hg (3–17 μg·kg$^{-1}$). In P#1, limestone was injected into the furnace and been calcined to CaO, which would interact with Hg in the flue gas to form the Hg$^p$ and subsequently been removed by ESP as particulates. Limestone in P#2 was inject into the WFGD tower as limestone slurry to react with gaseous SO$_2$ to form gypsum. Hg in gypsum of P#2 was only 12 $\pm$ 5 μg·kg$^{-1}$, this may be due to that most Hg in flue gas had been detained by ESP-FF in the upstream. Hg in fuels would be liberated into the flue gas under the combustion process in boilers and only few of Hg remained in the bottom ash [22]. Under the high combustion temperature (800–950 °C) and particulate circulation in CFB boilers, Hg content of bottom ash were 0 (below detection limit) μg·kg$^{-1}$ and 2.8 $\pm$ 2.4 μg·kg$^{-1}$ in P#1 and P#2, respectively. Hg in fly ash of P#1 was as high as 895 $\pm$ 42 μg·kg$^{-1}$, while the figures for ESP fly ash and FF fly ash in P#2 were 237 $\pm$ 6 μg·kg$^{-1}$ and 323 $\pm$ 13 μg·kg$^{-1}$, respectively.

Mercury relative enrichment factor (MREF), a parameter that describes trace element enrichment in fly ash or bottom ash relative to the feed coal [29], is defined as:

$$MREF = \frac{C_{ash} \times A_{ad}}{C_{coal}} \tag{1}$$

where $C_{ash}$ is Hg concentration in fly ash or bottom ash; $A_{ad}$ is ash yield of feed coal on air-dried basis; $C_{coal}$ is Hg concentration in feed coal.

Hg, a volatile element during coal combustion [29], was volatilized from feed coal and adsorbed onto and enriched in fly ash (MREF = 1.31–1.79, Table 3), while depleted in bottom ash (MREF = 0–0.02). It had been consistently observed that captured fly ash exceeded stack flue gas as the primary Hg output in recent studies for CFB utility boilers in China [21,30–33]. Factors influencing adsorption of Hg onto fly ash include particulate matter (PM) size, its structure and surface area [26], UBC content [34,35], flue gas

**Table 2**
Proximate and ultimate analysis of fuels.

| Power plants | Fuel type | Proximate analysis (%) | | | | Ultimate analysis (%) | | | | $Q_{net,ad}$ (MJ kg$^{-1}$) |
|---|---|---|---|---|---|---|---|---|---|---|
| | | $M_{ad}$ | $V_{ad}$ | $A_{ad}$ | $FC_{ad}$ | $C_{ad}$ | $H_{ad}$ | $N_{ad}$ | $S_{ad}$ | |
| P#1 | Coal (No. = 5) | 2.52 | 10.41 | 39.62 | 47.45 | 50.85 | 2.28 | 0.68 | 3.05 | 19.66 |
| P#2 | Coal slime (No. = 4) | 9.06 | 17.53 | 43.94 | 29.47 | 41.86 | 2.96 | 0.82 | 0.29 | 17.03 |
| | Gangue (No. = 4) | 2.89 | 18.77 | 45.15 | 33.19 | 47.24 | 3.21 | 0.85 | 0.45 | 19.29 |

Note: No., the number of samples; M, moisture; A, ash; V, volatile; FC, fixed carbon; C, carbon; H, hydrogen; N, nitrogen; O, oxygen; S, sulfur; Q$_{net}$, net calorific value; Subscript "ad", air-dried basis.

**Table 3**
Hg concentration in solid samples.

| P#1 | Hg ($\mu g \cdot kg^{-1}$) | MREF[*] | P#2 | Hg ($\mu g \cdot kg^{-1}$) | MREF[*] |
|---|---|---|---|---|---|
| Coal | 233 ± 39 (No. = 5)[**] | | Coal slime | 65 ± 20 (No. = 4) | |
| | | | Gangue | 113 ± 23 (No. = 4) | |
| Limestone | 17 ± 0 (No. = 1) | | Limestone | 4 ± 1 (No. = 4) | |
| Bottom ash | 0 ± 0 (No. = 5) | 0.00 | Bottom ash | 2.8 ± 2.4 (No. = 4) | 0.02 |
| Fly ash (ESP) | 895 ± 42 (No. = 5) | 1.52 | Fly ash (ESP) | 237 ± 6 (No. = 4) | 1.31 |
| | | | Fly ash (FF) | 323 ± 13 (No. = 4) | 1.79 |
| | | | Gypsum | 12 ± 5 (No. = 4) | |

  [*] MREF: mercury relative enrichment factor.
  [**] Hg content is expressed in arithmetic mean ± standard deviation.

compositions such as the halogen and sulfur [36,37], etc. Furthermore, the lower combustion temperature (800–950 °C) in CFB boiler than that in PC boiler (> 1400 °C) enhanced the activity of UBC that not been melted at the lower temperatures and possibly adsorbed more gaseous Hg ($Hg^0$ and $Hg^{2+}$) onto fly ash. The presence of CaO and high PM load in flue gas could further enhance the adsorption and facilitate in the $Hg^p$ formation in CFB boilers. In the present study, the average UBC content in fly ash of P#1 and P#2 was 4.97% and 2.63%, respectively, resulting in $Hg^p$ as the predominant species in the flue gas.

### 3.3. Mercury in flue gas and removals

Hg speciation and concentration in flue gas of the two investigated plants are shown in Table 4 and Fig. 2. In P#1, the flue gas temperature was maintained at 118–120 °C and total Hg (THg) in the flue gas dropped from 32.5 ± 10.4 $\mu g \cdot m^{-3}$ to 0.19 ± 0.04 $\mu g \cdot m^{-3}$ using the ESP. Impacted by the limestone slurry spray in WFGD, the temperature of flue gas decreased from 136 °C to 51 °C in P#2, and the THg level fell from 16.2 ± 3.1 $\mu g \cdot m^{-3}$ to 0.24 ± 0.06 $\mu g \cdot m^{-3}$ after ESP-FF + WFGD. THg concentration in the stack flue gas met the Hg emission standard for thermal power plants in China (30 $\mu g \cdot m^{-3}$, GB 13223-2011). The composition of Hg speciation in the flue gas of these two power plants was nearly the same (Table 4 and Fig. 2): both mainly comprised of $Hg^p$ (95.11–99.26%), followed by $Hg^{2+}$ (0.41–3.72%) and $Hg^0$ (0.33–1.17%) at the ESP inlet; while, $Hg^{2+}$ (47.91–50.17%) and $Hg^0$ (44.94–51.15%) were the predominant species in the outlet of ESP/WFGD, consistent with an earlier report showing the predominance of $Hg^{2+}$ and $Hg^0$ in Hg emissions from coal-fired power plants in China [31].

The removal efficiency of Hg by APCDs in the two CFB plants is shown in Table 5. A removal efficiency of 99.41% (ESP) and 98.53% (ESP-FF + WFGD) was achieved for THg in P#1 and P#2, respectively. Nearly all $Hg^p$ was captured by APCDs and retained as fly ash, with the particulate Hg removal efficiency of 99.97% and 99.99% in P#1 and P#2 (Table 5), respectively. Although $Hg^{2+}$ in the final discharged flue gas was both in a similar range of 0.10–0.12 $\mu g \cdot m^{-3}$, the removal efficiency of $Hg^{2+}$ in P#2 (81.21%) was much higher than that in P#1 (24.10%), indicating that WFGD in P#2 had a great removal effect on $Hg^{2+}$ [38]. Most of Hg in fuels was released into the flue gas as $Hg^0$ during the combustion, the addition of limestone in IFD significantly increased the particulate matter content in the flue gas [35], so gaseous Hg would be absorbed onto the particles as $Hg^p$ after temperature dropping drastically [39]. At the same time, this also mean that Hg in flue gas of P#1 was easy to remove, and the removal efficiency can reach to the same level as P#2 (ESP-FF + WFGD) when P#1 only had ESP but with IFD. Therefore, desulphurization facilities (IFD or WFGD) in power plants can produce a substantial co-benefit in Hg removal in addition to $SO_2$ scrubbing.

Table 6 shows a summary of recent report of Hg emission through stack flue gas from coal-fired power plants. Compared with other studies, Hg concentrations of flue gas observed in this investigation was at a low level, similar to the values reported by Wei et al. [40] and Teng

et al. [23]. Due to the Hg removal efficiency of the PC boiler power plants (27.5–97.7%, most below 80%) was lower than that of CFB boilers (74.0–99.41%, most above 80%), the exhaust gas from CFB boilers had less Hg than that of PC boilers (Table 6). The combustion temperature of CFB and PC boilers can reach 800–950 °C and over 1400 °C, respectively [39]. Although both type of boilers released substantial fraction of Hg (> 90%) into flue gas during combustion [22], the CFB boilers was more conducive to remove the total Hg in flue gas since the majority Hg in flue gas exist as the $Hg^p$ form which would be easily removed by ESP or FF [33,35,39]. This suggested that CFB boilers was in favor of Hg emission reduction when just equipped with dust collector.

### 3.4. Mercury mass balance and emission factors

A mass balance analysis was performed for the two power plants. The results are shown in Tables 7, 8 and Fig. 3. As the primary Hg input source for CFB boilers, fuels accounted 98.35% (389.3 $g \cdot d^{-1}$) and 99.95% (272.9 $g \cdot d^{-1}$) for THg input in P#1 and P#2, respectively. By comparison, the contribution from limestone was only 6.5 $g \cdot d^{-1}$ (1.65%) and 0.13 $g \cdot d^{-1}$ (0.05%), in P#1 and P#2, respectively. The temperature of combustion process in boilers was so high that little Hg remains in the bottom ash (< 0.56%). Hg in gypsum from WFGD de-sulphurization only accounted 0.24% of the THg output. However, most $Hg^p$, little $Hg^{2+}$ and $Hg^0$ were captured in the fly ash by ESP or ESP-FF. Compared with other Hg output (such as stack flue gas and gypsum), fly ash was the leading discharge pathway for CFB utility boilers, this was similar to Duan et al. [33], Zhao et al. [26], Burmistrz et al. [41] and Teng et al. [23]. Therefore, the disposal of such Hg-containing solid wastes must be carefully managed to prevent Hg re-emissions into the environment. Based on the total Hg data obtained from the output (bottom ash, fly ash, gypsum and flue gas) and input (fuel coal and limestone), Hg output/input ratio ranged from 101.38-103.67% in the two studied plants (Tables 7, 8), indicating reliable calculation of Hg mass balance.

Mercury emission factor (MEF), a parameter estimating Hg emissions from coal-fired power plants, is calculated based on the following three equations:

$$MEF_1 = \frac{M_{Hg}}{M_{coal}} \tag{2}$$

$$MEF_2 = \frac{M_{Hg}}{P \times t} \tag{3}$$

$$MEF_3 = \frac{M_{Hg}}{M_{coal} \times Q_{net,ad}} \tag{4}$$

where $MEF_1$, $MEF_2$ and $MEF_3$ are mercury emission factors based on the fuel consumption, electricity generated and heat value of fuel, respectively; $M_{Hg}$ is the amount of Hg released into the atmosphere per day ($g \cdot d^{-1}$); $M_{coal}$ is the consumption of fuel ($t \cdot d^{-1}$); $P$ is the actual power generated by tested power plant (110 MW and 183 MW for P#1 and P#2, respectively); $t$ is running time of generator (24 $h \cdot d^{-1}$); $Q_{net,ad}$ is

**Table 4**
Total and speciated Hg in the flue gas and associated parameters of the flue gas in the two tested CFB power plants.

| Power plants | Sampling location | Test number | Date | Time period | Sample Volume (m³) | Temperature (°C) | Moisture content (%, v/v) | $Hg^P$ (μg·m$^{-3}$) | $Hg^{2+}$ (μg·m$^{-3}$) | $Hg^0$ (μg·m$^{-3}$) | $THg$ (μg·m$^{-3}$) | Proportion of speciated Hg (%) | | |
|---|---|---|---|---|---|---|---|---|---|---|---|---|---|---|
| | | | | | | | | | | | | $Hg^P$ | $Hg^{2+}$ | $Hg^0$ |
| P#1 | ESP inlet | P#1-1 | 2014-08-26 | 12:50–14:02 | 0.94 | 117 | 4.93 | 25.0 | 0.13 | 0.11 | 25.2 | 99.05 | 0.51 | 0.44 |
| | | P#1-2 | 2014-08-26 | 15:20–16:34 | 0.99 | 119 | 4.30 | 39.7 | 0.12 | 0.09 | 39.9 | 99.46 | 0.31 | 0.23 |
| | | Mean ± SD | | | 0.97 ± 0.03 | 118 ± 1 | 4.62 ± 0.44 | 32.3 ± 10.4 | 0.13 ± 0.00 | 0.10 ± 0.01 | 32.5 ± 10.4 | 99.26 | 0.41 | 0.33 |
| | ESP outlet | P#1-1 | 2014-08-26 | 12:50–14:13 | 1.38 | 119 | 4.73 | 0.02 | 0.11 | 0.09 | 0.22 | 6.98 | 49.46 | 43.56 |
| | | P#1-2 | 2014-08-26 | 15:20–16:44 | 1.32 | 120 | 5.72 | 0.00 | 0.08 | 0.08 | 0.16 | 2.80 | 50.88 | 46.32 |
| | | Mean ± SD | | | 1.35 ± 0.04 | 120 ± 1 | 5.22 ± 0.70 | 0.01 ± 0.01 | 0.10 ± 0.02 | 0.09 ± 0.01 | 0.19 ± 0.04 | 4.89 | 50.17 | 44.94 |
| P#2 | ESP-FF inlet | P#2-1 | 2015-08-19 | 15:02–16:32 | 0.72 | 134 | 13.8 | 18.0 | 0.51 | 0.22 | 18.7 | 96.11 | 2.74 | 1.15 |
| | | P#2-2 | 2015-08-19 | 16:53–18:08 | 0.63 | 132 | 13.8 | 15.6 | 0.88 | 0.15 | 16.6 | 93.79 | 5.30 | 0.91 |
| | | P#2-3 | 2015-08-20 | 09:00–10:16 | 0.61 | 137 | 12.6 | 16.5 | 0.83 | 0.23 | 17.5 | 93.95 | 4.74 | 1.30 |
| | | P#2-4 | 2015-08-20 | 10:45–12:01 | 0.64 | 140 | 15.0 | 11.4 | 0.25 | 0.15 | 11.8 | 96.58 | 2.10 | 1.31 |
| | | Mean ± SD | | | 0.65 ± 0.05 | 136 ± 4 | 13.8 ± 0.99 | 15.3 ± 2.84 | 0.62 ± 0.30 | 0.19 ± 0.04 | 16.2 ± 3.1 | 95.11 | 3.72 | 1.17 |
| | WFGD outlet | P#2-1 | 2015-08-19 | 15:04–16:35 | 1.48 | 51 | 15.7 | 0.00 | 0.10 | 0.18 | 0.28 | 0.60 | 35.28 | 64.12 |
| | | P#2-2 | 2015-08-19 | 16:55–18:10 | 1.17 | 51 | 14.8 | 0.00 | 0.17 | 0.11 | 0.28 | 1.19 | 60.30 | 38.51 |
| | | P#2-3 | 2015-08-20 | 08:43–10:13 | 1.40 | 50 | 15.0 | 0.00 | 0.14 | 0.10 | 0.24 | 0.47 | 57.98 | 41.55 |
| | | P#2-4 | 2015-08-20 | 10:29–12:00 | 1.59 | 50 | 12.8 | 0.00 | 0.06 | 0.09 | 0.15 | 1.51 | 38.08 | 60.41 |
| | | Mean ± SD | | | 1.41 ± 0.18 | 51 ± 1 | 14.6 ± 1.22 | 0.00 ± 0.00 | 0.12 ± 0.05 | 0.12 ± 0.04 | 0.24 ± 0.06 | 0.94 | 47.91 | 51.15 |
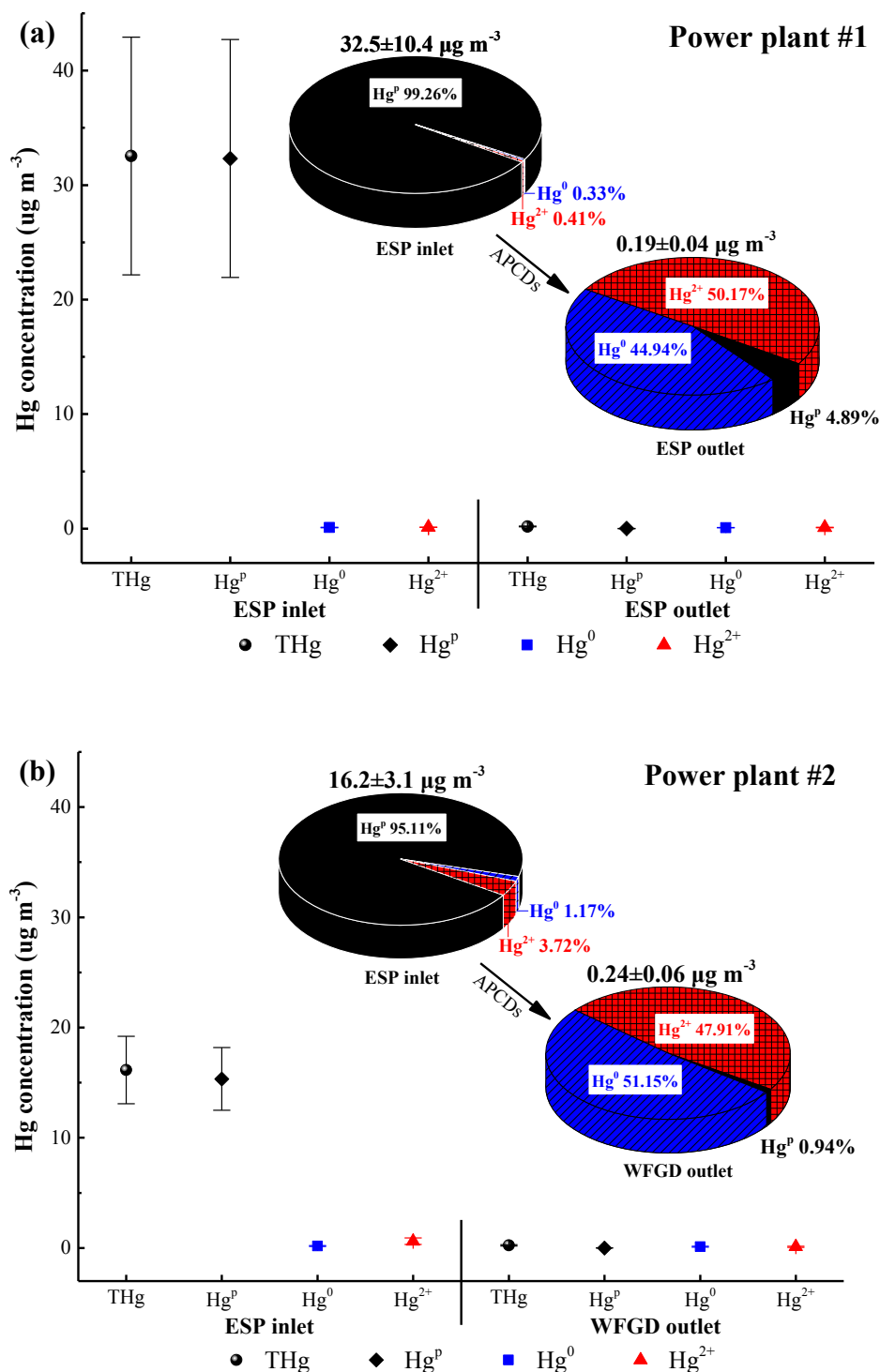
Fig. 2. Concentration and speciation of Hg in flue gas of two tested power plants.

**Table 5**
Removal efficiency of Hg in flue gas by the APCDs.

| Power plants | APCDs | $Hg^p$ (%) | $Hg^{2+}$ (%) | $Hg^0$ (%) | THg (%) |
|---|---|---|---|---|---|
| P#1 | ESP | 99.97 | 24.10 | 15.19 | 99.41 |
| P#2 | ESP-FF + WFGD | 99.99 | 81.21 | 36.46 | 98.53 |

calorific value of fuel ($MJ \cdot kg^{-1}$).

MEFs of tested CFB power plants are assessed in Tables 7 and 8. Compared the MEFs of coal-fired power plants reported in recent years

(Table 6), Hg release from the two CFB power plants (1.19–1.54 mg $Hg \cdot t^{-1}$ coal; 0.78–1.19 µg $Hg \cdot (kW \cdot h)^{-1}$; 0.06–0.08 g $Hg \cdot TJ^{-1}$) was far less than others. The MEFs can be influenced by the fuel types, APCDs, boiler types, flue gas compositions, etc. [24,31,41]. With the technological development of APCDs and the elimination of small and outdated boilers, significant progress had been made in China in the past decade for air pollutants control, including $NO_x$, $SO_2$ and PM. Based on the data collected in this study, Hg release from CFB power plants was also substantially reduced as a result of modern APCD implementation, showing much lower Hg emission compared to earlier reports. Attention to Hg release from coal fired power plants needs to be directed to the Hg re-emission/release from the

**Table 6**
Comparison of Hg emission data from coal-fired power plants.

| Geographical position | Boiler type | APCDs* | THg | Hg$^P$ | Hg$^{2+}$ | Hg$^0$ | Removal rate | Emission factors | Reference |
|---|---|---|---|---|---|---|---|---|---|
| Guizhou | CFB | IFD + ESP | 0.19 | 0.01 | 0.1 | 0.09 | 99.41% | 0.78 μg Hg·(kW·h)$^{-1}$ 1.19 mg Hg·t$^{-1}$ coal 0.06 g Hg·TJ$^{-1}$ | This study |
| Guizhou | CFB | SNCR + ESP-FF + WFGD | 0.24 | 0 | 0.12 | 0.12 | 98.53% | 1.19 μg Hg·(kW·h)$^{-1}$ 1.54 mg Hg·t$^{-1}$ coal 0.08 g Hg·TJ$^{-1}$ | This study |
| Shanxi | CFB | IFD + FF | – | – | – | – | 85–90% | 38.23 μg Hg·(kW·h)$^{-1}$ | [21] |
| Shanxi | CFB | SCR + FF + WFGD | – | – | – | – | 89.42% | 23.4 μg Hg·(kW·h)$^{-1}$ | [21] |
| Shanxi | CFB | IFD + ESP + FF | – | – | – | – | 85–90% | 18.11 μg Hg·(kW·h)$^{-1}$ | [21] |
| China | CFB | IFD + SNCR + ESP + WFGD | 2.05 | 0.09 | 0.1 | 2.01 | 83.02% | 0.69 g Hg·TJ$^{-1}$ | [24] |
| China | CFB | IFD + SNCR + FF + WFGD | 2.26 | 0 | 0.04 | 2.22 | 76.41% | 0.70 g Hg·TJ$^{-1}$ | [24] |
| China | CFB | IFD + SNCR + FF + WFGD | 2.49 | 0 | 0.04 | 2.58 | 74.72% | 0.80 g Hg·TJ$^{-1}$ | [24] |
| China | CFB | ESP | – | – | – | – | 74% | – | [22] |
| China | CFB | FF | – | – | – | – | 86% | – | [22] |
| China | CFB | SNCR + ESP-FF | 0.27 | – | – | – | 90.30% | – | [23] |
| China | CFB | SNCR + FF + WFGD | 0.3 | – | – | – | 83.80% | – | [23] |
| China | CFB | SNCR + FF + WFGD | 0.25 | – | – | – | 84.40% | – | [23] |
| China | CFB | SCR + FF + WFGD | 0.36 | – | – | – | 87.70% | – | [23] |
| China | CFB | FF + WFGD | 0.26 | – | – | – | 99.35% | – | [40] |
| Spain | CFB | ESP | 0.25 | – | 0.08 | 0.17 | | – | [42] |
| Spain | CFB | FF | 2.15 | – | 0.39 | 1.76 | – | – | [43] |
| China | PC | ESP + WFGD | 0.37 | – | – | – | 97.65% | – | [40] |
| Anhui | PC | ESP + WFGD | – | – | – | – | 36–46% | 0.27 g Hg·t$^{-1}$ coal | [27] |
| China | PC | SCR + ESP + WFGD | 3.75 | – | – | – | 88.54% | – | [44] |
| Guizhou | PC | SCR + ESP + WFGD | 0.6 | 0 | 0.11 | 0.49 | 97.56% | 3.87 mg Hg·t$^{-1}$ coal 2.54 μg Hg·(kW·h)$^{-1}$ | [45] |
| Guizhou | PC | ESP + WFGD | 6.69 | 0 | 1.66 | 5.03 | 67.80% | 75 mg Hg·t$^{-1}$ coal | [30] |
| Guizhou | PC | ESP + WFGD | 4.53 | 0 | 0.84 | 3.7 | 70.00% | 43 mg Hg·t$^{-1}$ coal | [30] |
| Guizhou | PC | ESP + WFGD | 5.06 | 0 | 0.45 | 4.61 | 81.40% | 32 mg Hg·t$^{-1}$ coal | [30] |
| Guangdong | PC | ESP + WFGD | 2.27 | 0 | 0.14 | 2.13 | 27.50% | 25 mg Hg·t$^{-1}$ coal | [30] |
| Beijing | PC | SCR + ESP + WFGD | 1.22 | 0 | 0.13 | 1.08 | 35.50% | 11 mg Hg·t$^{-1}$ coal | [30] |
| Inner Mongolia | PC | SCR + FF + WFGD | 0.57 | 0.01 | 0.03 | 0.53 | 96.20% | 8.71 kg Hg·y$^{-1}$ | [45] |
| Inner Mongolia | PC | SCR + ESP + WFGD | 3.8 | 0 | 0.42 | 3.39 | 77.74% | 60.28 kg Hg·y$^{-1}$ | [45] |
| Inner Mongolia | PC | SCR + ESP-FF + WFGD | 1 | 0 | 0.15 | 0.86 | 92.30% | 8.95 kg Hg·y$^{-1}$ | [45] |
| China | PC | SCR + ESP + WFGD + WESP | 4.3 | 0 | 0.3 | 4 | 56.59% | 1.56 g Hg·TJ$^{-1}$ | [26] |
| Poland | PC | ESP + WFGD | 2–5 | – | – | – | 65% | 0.71–1.80 g Hg·TJ$^{-1}$ | [41] |
| Poland | PC | ESP + WFGD | 15.1 | – | – | – | 60% | 6.09 g Hg·TJ$^{-1}$ | [41] |

 * IFD: In-furnace desulphurization; ESP: Electrostatic precipitator; SNCR: Selective non catalytic reduction; FF: Fabric filter; WFGD: Wet flue gas desulphurization; SCR: Selective catalytic reduction; WESP: Wet electrostatic precipitator; Unit of THg, Hg$^0$, Hg$^{2+}$ and Hg$^P$ were in μg·m$^{-3}$.

**Table 7**
Hg mass balance and emission factors of P#1.

| Hg input/output | Materials | Material flow rate (t·d$^{-1}$ for solid material/$10^4 \times$ m$^3$·d$^{-1}$ for flue gas) | Hg input/output (g·d$^{-1}$) | Percentage (%) |
|---|---|---|---|---|
| Hg input | Coal | 1730 | 389.30 | 98.35 |
| | Limestone | 384 | 6.54 | 1.65 |
| | Total | / | 395.84 | 100.00 |
| Hg output | Bottom ash | 240 | 0.00 | 0.00 |
| | Fly ash | 446 | 399.25 | 99.49 |
| | Flue gas | 1087 | 2.06 | 0.51 |
| | Total | / | 401.31 | 100.00 |
| Hg output/input ratio | 101.38% | | | |
| MEF based on fuel | 1.19 mg Hg·t$^{-1}$ coal | | | |
| MEF based on electricity* | 0.78 μg Hg·(kW·h)$^{-1}$ | | | |
| MEF based on calorific value | 0.06 g Hg·TJ$^{-1}$ | | | |

 * Actual output power: 110 MW.

captured fly ash.

**Table 8**
Hg mass balance and emission factors of P#2.

| Hg input/output | Material | Material flow rate (t·d$^{-1}$ for solid material/$10^4 \times$ m$^3$·d$^{-1}$ for flue gas) | Hg input/output (g·d$^{-1}$) | Percentage (%) |
|---|---|---|---|---|
| Hg input | Gangue | 1070 | 120.85 | 44.26 |
| | Coal slime | 2339 | 152.04 | 55.69 |
| | Limestone | 36 | 0.13 | 0.05 |
| | Total | / | 273.02 | 100.00 |
| Hg output | Bottom ash | 563 | 1.58 | 0.56 |
| | Fly ash* | 1120 | 275.52 | 97.35 |
| | Gypsum | 58 | 0.69 | 0.24 |
| | Flue gas | 2213 | 5.24 | 1.85 |
| | Total | / | 283.03 | 100.00 |
| Hg output/input ratio | 103.67% | | | |
| MEF based on fuel | 1.54 mg Hg·t$^{-1}$ coal | | | |
| MEF based on electricity** | 1.19 μg Hg·(kW·h)$^{-1}$ | | | |
| MEF based on calorific value | 0.08 g Hg·TJ$^{-1}$ | | | |

 * Fly ash from ESP and FF account for 90% and 10%, respectively, and with weighted Hg content of 246 μg·kg$^{-1}$.
 ** Actual output power: 183 MW.

## 4. Conclusions

Characterization of Hg emissions from CFB coal-fired power plants with different fuels and APCDs in Southwest China leads to the following conclusion:

(1) The stack flue gas from P#1 and P#2 had Hg concentrations measured by OHM of 0.19 μg·m$^{-3}$ and 0.24 μg·m$^{-3}$, respectively. Observed Hg speciation was: Hg$^0$ (44.94–51.15%) and Hg$^{2+}$ (47.91–50.17%), followed by Hg$^P$ (0.94–4.89%).

(2) The Hg removal efficiency of APCDs was in the range of
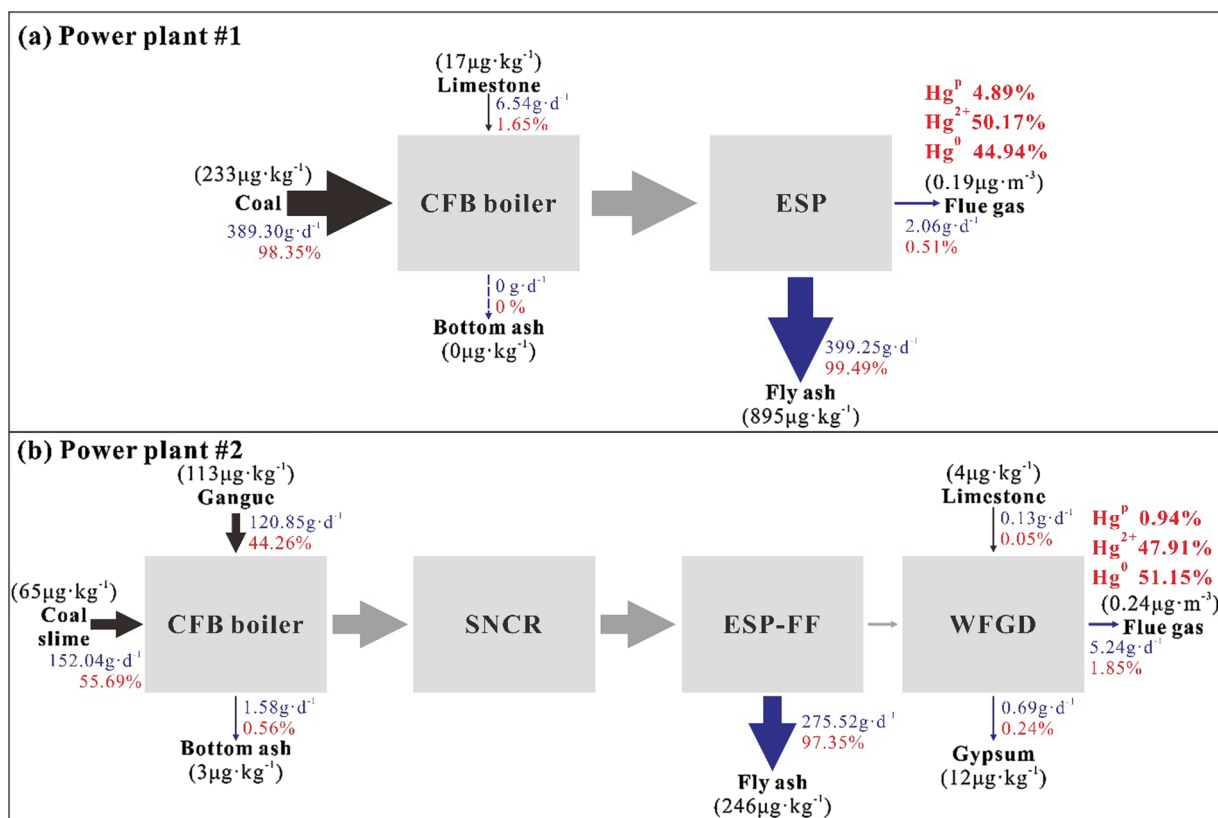
**Fig. 3.** Mass balance diagrams of Hg observed in the two CFB power plants.

98.53–99.41%, with most (> 97%) was removed by dust collector. As a consequence, MEFs were as low as 1.19–1.54 mg Hg·t$^{-1}$ coal; 0.78–1.19 μg Hg·(kW·h)$^{-1}$; 0.06–0.08 g Hg·TJ$^{-1}$.

(3) The Hg output/input ratio ranged from 101.38 to 103.67%. Hg in the two CFB coal-fired plants came primarily from fuel (98.35–99.95%) and escaped mainly through the captured fly ash (97.35–99.49%). Besides, the Hg input from limestone and output from bottom ash and gypsum were in an extreme low level.

(4) The MEFs estimated from the data collected in the two tested power plants were lower than the reports from earlier studies, suggesting that Hg emission data from CFB coal-fired power plants need to be further updated.

## Acknowledgements

## References

[1] UNEP. Global mercury assessment 2013: sources, emissions, releases and environmental transport. Geneva, Switzerland: UNEP Chemicals Branch; 2013.

[2] World Health Organization (WHO). Environmental health criteria. Inorganic mercury. Geneva: World Health Organization; 1991.

[3] Pacyna EG, Pacyna JM. Global emission of mercury from anthropogenic sources in 1995. Water Air Soil Pollut 2002;137:149–65.

[4] Pacyna EG, Pacyna JM, Steenhuisen F, Wilson S. Global anthropogenic mercury emission inventory for 2000. Atmos Environ 2006;40:4048–63.

[5] Pacyna EG, Pacyna JM, Sundseth K, Munthe J, Kindbom K, Wilson S, et al. Global emission of mercury to the atmosphere from anthropogenic sources in 2005 and

[6] Antonio J, Martín R, Nanos N. Soil as an archive of coal-fired power plant mercury deposition. J Hazard Mater 2016;308:131–8.

[7] Li ZG, Feng XB, Li GH, Bi XY, Sun GY, Zhu JM, et al. Mercury and other metal and metalloid soil contamination near a Pb/Zn smelter in east Hunan province China. Appl Geochem 2011;26(2):160–6.

[8] Li XY, Li ZG, Lin C-J, Bi XY, Liu JL, Feng XB, et al. Health risks of heavy metal exposure through vegetable consumption near a large-scale Pb/Zn smelter in central China. Ecotoxicol Environ Saf 2018;161:99–110.

[9] Xu XH, Meng B, Zhang C, Feng XB, Gu CH, Guo JY, et al. The local impact of a coal-fired power plant on inorganic mercury and methyl-mercury distribution in rice (Oryza sativa L.). Environ Pollut 2017;223:11–8.

[10] Streets DG, Horowitz HM, Jacob DJ, Lu ZF, Levin L, Schure AFH, et al. Total mercury released to the environment by human activities. Environ Sci Technol 2017;51:5969–77.

[11] UNEP. Global mercury assessment. Geneva, Switzerland. 2002.

[12] Wu Y, Wang SX, Streets DG, Hao JM, Chan M, et al. Trends in anthropogenic mercury emissions in china from 1995 to 2003. Environ Sci Technol 2006;40(17):5312–8.

[13] Wu QR, Wang SX, Li GL, Liang S, Lin C-J, Wang YF, et al. Temporal trend and spatial distribution of speciated atmospheric mercury emissions in China during 1978–2014. Environ Sci Technol 2016;50:13428–35.

[14] Zhang L, Wang SX, Wang L, Wu Y, Duan L, Wu QR, et al. Updated emission inventories for speciated atmospheric mercury from anthropogenic sources in China. Environ Sci Technol 2015;49(5):3185–94.

[15] Yue GX, Lu JF, Xu P, Hu XK, Ling W, Chen Y, et al. The up-to-date development and future of circulating fluidized bed combustion technology. Electric Power 2016;49(1):1–13. (In Chinese with English abstract).

[16] Xiang BX, Li JF, Yang HR, Lv JF. The operation analysis of medium-sized circulating fluidized bed boiler units. Boiler Technol 2016;46(5). 31-9,46. (In Chinese with English abstract).

[17] Liu KY, Wang SX, Wu QR, Long W, Qiao M, Zhang L, et al. A highly resolved mercury emission inventory of Chinese coal-fired power plants. Environ Sci Technol 2018;52(4):2400–8.

[18] Dai SF, Ren DY, Chou CL, Finkelman RB, Seredin VV, et al. Geochemistry of trace elements in Chinese coals: a review of abundances, genetic types, impacts on human health, and industrial utilization. Int J Coal Geol 2012;94:3–21.

[19] Yudovich YE, Ketris MP. Mercury in coal: a review: part 1 geochemistry. Int J Coal Geol 2005;62(3):107–34.

[20] Huang Y, Deng MH, Li TQ, Japenga J, Chen QQ, Yang XE, et al. Anthropogenic mercury emissions from 1980 to 2012 in China. Environ Pollut 2017;226:230–9.

[21] Gao LB, Wang YP, Huang QW, Guo SQ. Emission of mercury from six low calorific value coal-fired power plants. Fuel 2017;210:611–6.

[22] Hui ML, Lei Z, Wang ZG, Wang SX. The mercury mass flow and emissions of coal-

fired power plants in China. China Environ Sci 2015;35(8):2241–50. (In Chinese with English abstract).

[23] Teng Y, Li XH, Su YJ, Zheng Y, Wang GY, Zhang K. Mercury emission characteristics of a circulating fluidized bed coal fired power plant based on field measurements. The proceedings of the twenty-first air pollution control technology symposium. 2017. p. 315–20. (In Chinese with English abstract).

[24] Cui J, Duan LB, Jiang Y, Zhao CS, Anthony EJ. Migration and emission of mercury from circulating fluidized bed boilers co-firing petroleum coke and coal. Fuel 2017;215:638–46.

[25] Bai XF, Ding H, Lian JJ, Ma D, Yang XY, et al. Coal production in China: past, present, and future projections. Int Geol Rev 2018;60(5–6):535–47.

[26] Zhao SL, Duan YF, Yao T, Liu M, Lu JH, Tan HZ, et al. Study on the mercury emission and transformation in an ultra-low emission coal-fired power plant. Fuel 2017;199:653–61.

[27] Chen BY, Liu GJ, Sun RY. Distribution and fate of mercury in pulverized bituminous coal-fired power plants in coal energy-dominant Huainan City, China. Arch Environ Contam Toxicol 2016;70(4):724–33.

[28] Zheng LG. Environmental geochemistry of mercury in coal. (Doctor Thesis). Anhui, China: University of Science and Technology of China; 2008. (In Chinese with English abstract).

[29] Meij R. Trace element behavior in coal-fired power plants. Fuel Process Technol 1994;39:199–217.

[30] Wang SX, Zhang L, Li GH, Wu Y, Hao JM, Pirrone N, et al. Mercury emission and speciation of coal-fired power plants in China. Atmos Chem Phy 2010;10(3):1183–92.

[31] Zhang L, Wang SX, Meng Y, Hao JM. Influence of mercury and chlorine content of coal on mercury emissions from coal-fired power plants in China. Environ Sci Technol 2012;46(11):6385–92.

[32] Chen L, Duan Y, Zhuo Y, Yang L, Zhang L, Yang X, et al. Mercury transformation across particulate control devices in six power plants of China: the co-effect of chlorine and ash composition. Fuel 2007;86:603–10.

[33] Duan YF, Zhuo YQ, Wang YJ, Zhang L, Yang GL, et al. Mercury emission and removal of a 135MW CFB utility boiler. Proceedings of the 20th international conference on fluidized bed combustion. Springer Berlin Heidelberg; 2010. p. 189–94.

[34] Yang GL, Duan YF, Fan XX. Enrichment characteristics of mercury in solid products of coal-fired power plants and influencing factors. J Combust Sci Technol 2010;6(16):485–90.

[35] Duan YF, Jiang YM, Yang LG, Wang YJ. Experimental study on mercury emission and adsorption in circulating fluidized bed boiler. Proc CESS 2008;28(32):1–5. (In Chinese with English abstract).

[36] Wang YJ, Duan YF, Yang LG, Zhao CS, Shen XL, Zhang MY, et al. Experimental study on mercury transformation and removal in coal-fired boiler flue gases. Fuel Process Technol 2009;90(5):643–51.

[37] Wang SM, Zhang YS, Gu YZ, Wang JW, Liu Z. Using modified fly ash for mercury emissions control for coal-fired power plant applications in China. Fuel 2016;181:1230–7.

[38] Liu YK, Zhuo YQ, Chen CH, Xu XC. Mercury removal performance of desulfurization systems in coal-fired power plants. Electr Power 2011;44(12):68–72. (In Chinese with English abstract).

[39] Yin LB, Zhuo YQ, Xu QS, Zhu ZW, Du W, An ZY. Mercury emission from coal-fired power plants in China. Proc CSEE 2013;33(29):1–9. (In Chinese with English abstract).

[40] Wei SQ, Teng Y, Li XH, Su YJ, Yang W, Zhang K. Comparison of mercury emission from around 300 mw coal-fired power generation units between pulverized boiler and circulating fluidized-bed boiler. J Fuel Chem Technol 2017;45(8):1009–16. (In Chinese with English abstract).

[41] Burmistrz P, Kogut K, Marczak M, Zwoździak J. Lignites and subbituminous coals combustion in Polish power plants as a source of anthropogenic mercury emission. Fuel Proc Technol 2016;152:250–8.

[42] López-Antón MA, Díaz-Somoano M, Diaz L, Martínez-Tarazona MR. Avoiding mercury emissions by combustion in a Spanish circulating fluidized-bed combustion (CFBC) plant. Energy Fuel 2011;25(7):3002–8.

[43] Font O, Córdoba P, Leiva C, Romeo LM, Bolea I, Guedea I, et al. Fate and abatement of mercury and other trace elements in a coal fluidised bed oxy combustion pilot plant. Fuel 2012;95:272–81.

[44] Li CF, Duan YF, Tang HJ, Zhu C, Zheng YW, Huang TF. Mercury emissions monitoring in a coal-fired power plant by using the EPA method 30b based on a calcium-based sorbent trap. Fuel 2018;221:171–8.

[45] Tang SL, Wang LN, Feng XB, Feng ZH, Li RY, Fan HP, et al. Actual mercury speciation and mercury discharges from coal-fired power plants in Inner Mongolia, northern China. Fuel 2016;180:194–204.